Current Applied Physics 32 (2021) 98–105

Contents lists available at ScienceDirect

Current Applied Physics

journal homepage: www.elsevier.com/locate/cap

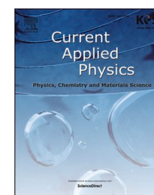

Electronic-beam evaporation processed titanium oxide as an electron selective contact for silicon solar cells

Vladyslav Matkivskyi [a], Youngseok Lee [b,*], Hyeon Sik Seo [b], Doh-Kwon Lee [c], Jong-Keuk Park [b], Inho Kim [b,**]

[a] Department of Material Science and Engineering, Norwegian University of Science and Technology (NTNU), Realfagbygget, Trondheim, Norway
[b] Center for Electronic Materials, Korea Institute of Science and Technology, Seoul, 02792, Republic of Korea
[c] Photo-electronic Hybrids Research Center, Korea Institute of Science and Technology, Seoul, 02792, Republic of Korea

ARTICLE INFO

Keywords:
Carrier selective contacts
Solar cells
TiO_2
e-beam
Passivation

ABSTRACT

This work is dedicated to the study of electronic-beam (e-beam) evaporated titanium oxide (TiO_x) contact for polycrystalline silicon hetero-junction solar cells. A TiO_x material obtained by e-beam evaporation method is suggested as a possible alternative to the atomic layer deposition (ALD) process. The purpose is to achieve corresponding passivation efficiency between e-beam evaporation of TiOx and the ALD method. However, the TiOx in question achieved a relatively low passivation performance of $S_{eff} = 113$ cm^{-1} in comparison to the reported ALD results. Nonetheless, as e-beam evaporation is well-established and an environmentally friendly deposition technology, e-beam evaporated TiO_x passivation layer has potential for improvement. What is clearly demonstrated in our work is how such an improvement in contact resistance dropped from >55 Ω/cm^2 to 2.29 Ω/cm^2. Indeed, our study established a correlation between the main process parameters of e-beam evaporation and their influence on the quality of electron selective TiO_x layer. Moreover, we reveal a possible scenario for the implementation of e-beam evaporated Titanium oxide as electron selective contact for asymmetrical hetero-junction solar cells.

1. Introduction

In the upcoming decade, it is likely there will be a noticeable switching period in the Si solar cell industry from homo-junction cells to hetero-junction technology. The Auger recombination and optical loss in heavily doped emitters in homo-junction cells remain unresolved. Therefore, the silicon hetero-junction (SHJ) structure or carrier selective contacts (CSC) structure that can structurally avoid these problems is attracting attention as a next-generation solar cells technology [1]. The SHJ solar cells with implemented doped amorphous silicon (a-Si) and intrinsic a-Si layers show the highest efficiency indexes on the photovoltaics (PV) market (Kaneka corp. – 26.7%) among the c-Si solar cells [2]. At the same time, the industry has drawbacks of a-Si application: Firstly, process cost of the a-Si material fabrication is relatively high, and secondly this material has low thermal stability and hole-carrier mobility in addition to the high resistance of undoped a-Si layers. Even though the market is deluged with Si-based materials, a-Si still shows the high quality of passivation and has wider bandgap than c-Si (Fig. 1(b)), which makes it preferable for the solar cell fabrication [3]. However, doped a-Si layer is limited by the doping process due to high fabrication costs and absorption losses in the doped material. Meanwhile, the PV research industry shows new approaches and materials to evade previously mentioned issues. One of such innovations in the solar cell developing is dopant free cells. The working principle of such photovoltaics is based on the formation of the p-n junction by application of materials with high range difference in the work functions (WF). Further carrier separation is based on the sharp contrast in the energy level of materials and silicon with the complete absence of emitter or back surface field – highly doped Si layers for the same application (Fig. 1(a)).

Consequently, such an approach gives the possibility to avoid the use of a-Si layers and introduce new materials in solar cell processing. Among alternative materials, metal oxides showed the most tunable and suitable properties for dopant free solar cells. The metal oxides were

* Corresponding author.
** Corresponding author.
E-mail addresses: yslee@kist.re.kr (Y. Lee), inhok@kist.re.kr (I. Kim).

https://doi.org/10.1016/j.cap.2021.10.005
Received 15 March 2021; Received in revised form 10 September 2021; Accepted 11 October 2021
Available online 20 October 2021
1567-1739/© 2021 The Authors. Published by Elsevier B.V. on behalf of Korean Physical Society. This is an open access article under the CC BY-NC-ND license (http://creativecommons.org/licenses/by-nc-nd/4.0/).

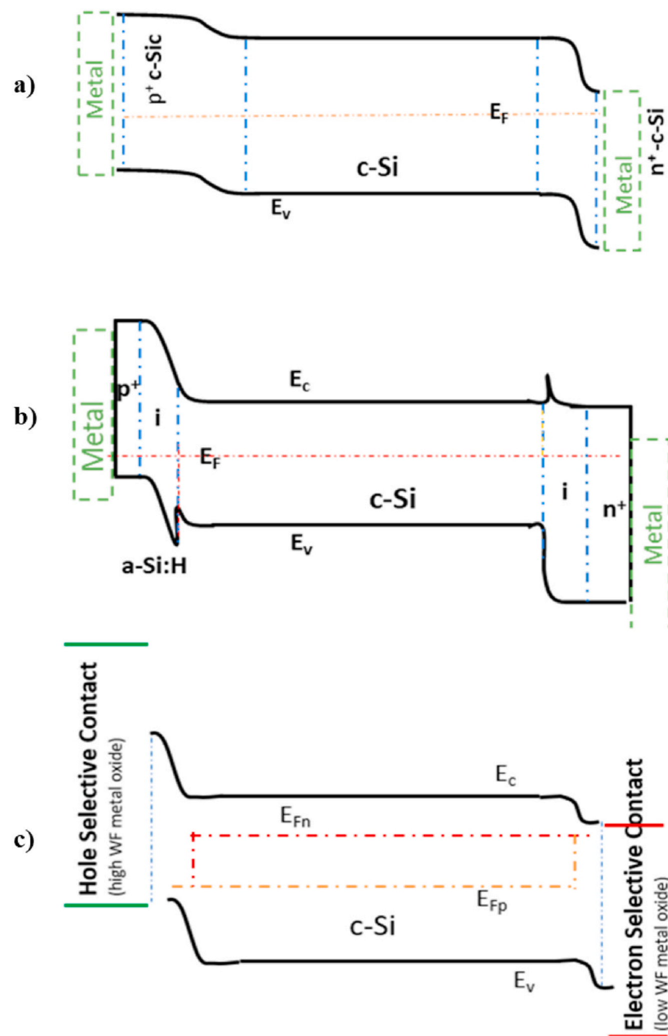

Fig. 1. Schematic of electronic band diagram in dark at equilibrium for (a) homo-junction solar cell, (b) hetero-junction solar cell with a-Si:H, (c) dopant free asymmetrical heterojunction solar cell (not to scale).

used in the industry previously [4] and in tandem with highly doped Si layers achieved considerable results: VO_x as hole selective contact for hetero-junction cell – 15.8% efficiency and V_{oc} = 606 mV [5]; hybrid hetero-junction cell with a-Si layers and TiO_x – electron selective layer and MoO_x – hole selective layer and for additional passivation showed PCE - 20.7% and V_{oc} = 706 mV [6]; NiO – hole selective contact in perovskite cell – 14.9% [7].

As a result, the widespread concept of using such materials for passivation and carrier separation brings us to the concept of carrier selective contacts (CSC) for c-Si solar cells. These materials have an electron selective or hole selective properties depending on their work function. This concept of CSC is also referred to as a dopant-free asymmetric heterojunction (DASH) solar cells as shown in Fig. 1(c). The photovoltaic industry is paying keen attention to the dopant-free cell capable of solving an emitter doping process (Auger recombination), which is one of the main limiting factors of conventional solar cells. The next step is to select materials for this approach to find the most reliable and repeatable conditions for implementation for the latest technologies and industries.

Titanium oxide is a well-known material in the semiconductor industry as TCO [8]. What makes titanium oxide attractive for the solar cell industry is the optical properties of this material, as it has a variety of positive qualities such as high refractive index, tunable work function from 3.0 eV up to 3.5 depending on the crystal phase of material [9] and chemical stability. Furthermore, the titanium oxide thin film layer was previously used as antireflection coating (ARC) [10] for c-Si solar cells and was also incorporated as an electron transport layer in the next generation solar cells such as perovskite solar cells [11]. The current semiconductor industry provides a vast choice of the titanium oxide material synthesis processes: atomic layer deposition (ALD) [12], magnetron sputtering [13], sol-gel method [14] or cathodic arc plasma deposition (CAPD) [15]. In order to obtain different material properties for various applications of titanium oxide material (TiO_x), all of these processes have been reported. TiO_x has become well known as transition metal oxide in the same line with other materials such as NiO [16], MoO_x [17], VO_x [18], WO_x [19] with the ability of carrier selection.

E-beam evaporated titanium oxide for passivation in Si solar cells has not been widely reported yet, as the ALD method seems to be well established and allows improved control of the deposition process. On the other hand, the ALD process needs precursor chemicals which are hazardous to the environment or human health: TiI_4 [20], $[Ti(OPri)_4]$ [21], Titanium isopropoxide (TTIP) [5]. Moreover, fabrication of such materials consists of complicated and expensive processing. Thus, there continues to be a need to identify more cost-effective and environment-friendly processes for TiO_x deposition.

E-beam evaporation is also a well-known technique for thin-film deposition [22]. High vacuum use and high throughput isolated from the outer environment set apart e-beam evaporation as a necessary technique in semiconductor processing. In the case of TiO_x, such an evaporation process makes it possible to avoid toxic and hazardous chemical consumption. Hence, this process provides deposition of thin titanium oxide films by evaporation of titanium oxide from the bulk material source by a melting of the source. In our work, we performed all deposition processing in high vacuum e-beam evaporation.

Our work approach is dedicated to the developing carrier selective contact based on the e-beam evaporated TiO_x thin film for the DASH cell. Based on this, under study TiO_x film needs to obtain excellent passivation and low resistivity for carrier transport through a specific layer to the metal contact. Base physical parameters which might be extracted from the material analysis is surface saturation current density J_0 [3] as passivation quality parameter. On the other hand, the description of conductivity via CSC contact layer can be treated as specific contact resistivity – ρ_{spc} [3].

2. Experimental methods

Experiments were performed on CZ c-Si n-type wafers, (100) crystal orientation, one-side polished with resistivity 1–5 Ω cm and thickness 520 ± 25 μm. Before cleaning, the wafers were laser sliced into square pieces by 1.5 cm × 1.5 cm. The next step involved etching in $HF:HNO_3$: Acetic acid (HNA) solution for the removal of the damaged silicon layer. After the etching samples were cleaned in RCA1 and RCA2 solutions and dried by N_2 blowers, they were placed on the holder for deposition. Following deposition, the samples proceeded to quality analysis of the deposited TiO_x.

The main research interest of our work is to find the feasibility of e-beam evaporated TiO_x as a promising alternative to the ALD deposited one, for achieving high passivation performance for the c-Si surface. Optimization of the e-beam evaporation equipment in our case has been achieved through the control of TiO_x deposition rate and base pressure during deposition. The evaporation process of TiO_x was performed at 5×10^{-6}–8×10^{-5} Torr and as evaporation source TiO_2 pallets of 1–5 mm size were used. During deposition, the thickness of the TiO_x thin films were controlled and an e-beam gun current was set at a range of 18–45A. Annealing of deposited TiO_x thin films was performed in the tube furnace at a temperature range of 100–550 °C.

Determination of passivation quality for TiO_x film was conducted through minority carrier lifetime (MCLT) measurements by photo conductance decay technique using an μ-PCD instrument (MDPspot by Freinberg Instruments). Following equipment measurements, MCLT

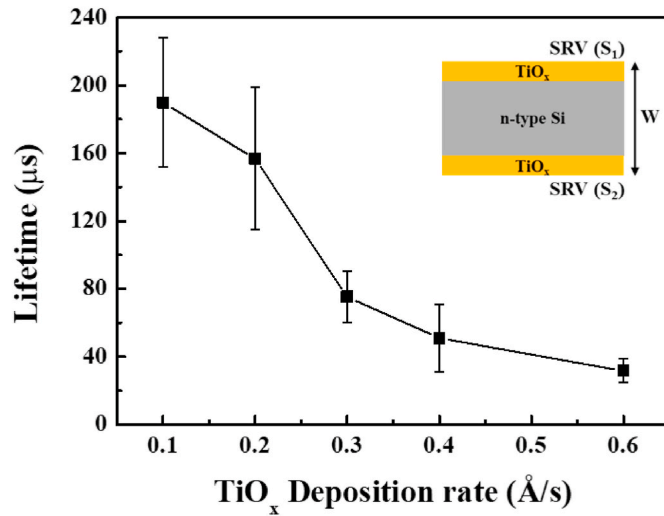

Fig. 2. The dependency of obtained MCLT and titanium oxide deposition rate performed during experiments and example of a fabricated sample in our work for MCLT measurements (top corner).

data can be converted to the surface recombination velocity (SRV) by the following equations (1)–(3).

$$\frac{1}{\tau_{eff}}=\frac{1}{\tau_b}+\frac{1}{\tau_s} \quad [1]$$

$$\frac{1}{\tau_s}=\frac{2S}{W}+\frac{1}{D}\left(\frac{W}{\pi}\right)^2 \quad [2]$$

$$S=\frac{W}{2}+\left(\frac{\tau_b+\tau_{eff}}{\tau_{eff}\tau_b}\right) \quad [3]$$

Where τ_{eff} – effective lifetime, a value obtained from the u-PCD measurement, τ_b – bulk lifetime, collected from the measuring bare n-type silicon wafer in iodine passivation of the bare wafer without TiO_x deposited layer, τ_s – surface minority carrier lifetime and W – overall thickness of sample. As both surfaces are passivated by the same material and same thickness, consequently $S = S_1 + S_2$, S, S_1, S_2 – are surface recombination velocities (SRV). Regarding the given equations (1) and (2) are valid for our case when c-Si wafers are coated with TiO_x on the front and rear side. A detailed sketch of the sample prepared for MCLT measurements is shown in Fig. 2.

For the contact resistance measurements of the TiO_x/n-Si contact, an Al layer with 200 μm thickness was deposited onto the samples. The transmission line method (TLM) [23] was applied to calculate specific contact resistance (ρ_{spc}), to achieve this an Al layer was deposited in a different line pattern (Fig. S1). Where Z represents the width of a particular Al pad, L corresponds to the length between each of them. R_c or contact resistance for the conducting material, TiO_x layer in our case.

Specific contact resistance (ρ_{spc}) of the layer was extracted by TLM and transferred to a slope, where sheet resistance of the layer (R_{sh}) is the function of so-called "transfer length" L_T (the average distance that charge carriers travel underneath the contact pad). A detailed methodology of TLM and graph plotting for f(R_{sh}) = LT is represented in the schematic Fig. S1 in the supplementary materials.

It is important to note that for the case under question, the following equations (4)–(6) are valid only when transfer length L_{Tx} is shorter than L_x. Hence, it is possible to estimate an approximate sheet resistance for the TiO_x thin film by the slopes obtained. In addition, R_{sh} is converted into specific contact resistance (ρ_{spc}) by the equations given below:

$$R_c=\frac{\rho_{spc}}{L_T Z}=\frac{R_{sh}}{L_T Z} \quad [4]$$

$$\rho_{spc}=\frac{L_T R_c}{Z} \quad [5]$$

$$L_T=\sqrt{\frac{\rho_{spc}}{R_{sh}}} \quad [6]$$

Further detailed crystallinity analysis of the deposited TiO_x passivation carrier-selective layer was conducted by Transmission Electron Microscopy (TEM, Titan 80–300 by FEI). The TEM analysis was performed on the three types of samples: i) an as-deposited 5 nm thin film of TiO_x, ii) an annealed TiO_x thin film (5 nm) at 450 °C, iii) a TiO_x 5 nm thin film with Al layer on top annealed at 400 °C.

Following the measurements of MCLT, specific data were transformed to the saturation current density parameter - J_0 by extracting it from equations (3) and (8). J_0 plays a crucial role in the determination of V_{oc} as described by equations (7) and (8), where S_{eff} is an effective surface recombination velocity attributed to the Shockley Read Hall (SRH) recombination, bandgap narrowing recombination, and front/back surface recombination. However, it does not include Auger recombination as we do not have a heavily doped emitter layer according to the DASH cell concept. In accordance with the further equations N_d – donor carrier concentration, Δn – excess carrier concentration, J_{sc} – short circuit current, q – elementary charge, T – temperature (K), k – Boltzmann constant, p – bulk minority carrier concentration, for the n-type Si. Regarding J_0, it can be extracted from the emitter saturation velocity (S_{eff}) which describes recombination losses for dopant free case $N_d \gg \Delta n$.

$$V_{OC}=\frac{nkT}{q}\ln\left(\frac{J_{sc}}{J_0}+1\right) \quad [7]$$

$$S_{eff}=\frac{J_0\left(N_d+\Delta n\right)}{p_i^2 q} \quad [8]$$

XRD (X-ray diffraction, D8-GADDS by Bruker) measurements were conducted in our study of TiO_x thin film composition analysis of as-deposited and annealed films. Furthermore, to unveil the origin of the contact resistance phenomena, conductive mode AFM (Atomic Force Microscopy, XE-70 by Parks Systems) was carried out on the samples.

3. Results and discussion

As previously mentioned, our approach is based on the e-beam deposition of carrier selective and passivation thin film of TiO_x by the e-beam evaporation. The deposition process effect on the quality of TiO_x thin film by deposition parameters was studied for the e-beam evaporator system environment. During the deposition, the e-beam gun current and deposition rate of TiO_x was controlled. It was discovered that current amplification increases the deposition rate of TiO_x. Furthermore, it was found that e-beam current affects the base pressure in the chamber, this can be interpreted as an example of evidence for possible change in the oxygen composition ratio in TiO_x thin film. This assumption is made from the results of the TiO_x deposition rate control experiment, where passivation quality of the deposited films with a different rate and post-annealing were studied, as shown in Fig. 2. According to the results obtained, we estimated a precise correlation between e-beam deposition rate control and the passivation quality of received TiO_x thin films (Fig. 2). Further, the change in base pressure during deposition depending on the e-beam gun current was investigated. Consequently, from the presented data in Fig. S2, we can comment that a possible reason for passivation quality suppression for films deposited at higher deposition rate is due to oxygen deficiency in TiO_x thin film. For a clearer understanding of such phenomena, a study of composition and stoichiometry analysis should be conducted for different deposition conditions. As our study is largely based on the post-deposition processing for passivation property improvement of titanium oxide thin films, closer investigation of such behavior in further works

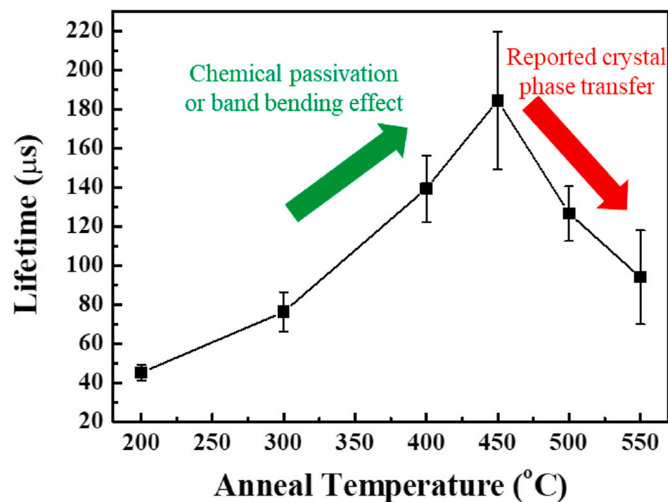

Fig. 3. The dependency of measured MCLT and post-deposition annealing temperature for 4 nm layer of TiO_x.

dedicated to the e-beam deposition process of TiO_x thin films needs investigation. Correspondingly with deposition rate analysis, the co-relation between the change of process parameters such as gun current and chamber base pressure was discovered. As this was partly revealed during deposition experiments, an increasing of e-beam gun current entails base chamber pressure changes which affect the deposition rate of TiO_x. Furthermore, a straight correlation between e-beam current with deposition rate and the growth of deposition rate as a function of gun current on the whole graph (Fig. S2) are observed.

The annealing procedure for deposited TiO_x thin film showed an explicit reliability on surface passivation improvement after the process dependent on the temperature. Such an experiment for the thermal influence control on the passivation quality of TiO_x thin films was carried out due to low minority carrier lifetime of as-deposited samples. What's more, such phenomena were reported previously during the work on the Ti oxidation where minority carrier lifetime was increased by the annealing [19]. According to this information, it was decided to expose samples with deposited TiO_x thin films to the annealing at different temperatures. At this juncture, a dramatic increase in the lifetime measurements after low-temperature annealing of deposited TiO_x thin films was witnessed. Furthermore, for our case critical temperature for improvement of passivation the TiO_x layer was found, as shown in Fig. 3, additionally at 450 °C lifetime of the samples decreases. Certain phenomena might be caused by the crystal phase formation in the TiO_x film, as titanium oxide has three different phases [24] and TiO_x material crystallization might be induced by the thermal annealing [25,26]. Additionally, secondary TEM analysis was performed to prove this theory or to reveal other reasons for such behavior of the TiO_x thin film. A phase change in TiO_x layer during the annealing in between 400–500 °C was observed by the TEM, it is indicated in Fig. 4. According with TEM and annealing experiment data, it is determined that for samples annealed at low temperatures (100, 200, 300, 400 °C) and without annealing, no phase change was observed. However, is it possible that phase-changes in material at 500 °C degrees became critical for the passivation quality of the TiO_x thin film. The evidence of phase transformation areas from amorphous to crystalline TiO_x are represented in Figs. 4 and 6

Following the TEM analysis data, a possible phase state of transformed areas was determined. Gatan Microscopy Suite Software was used to estimate the lattice parameter of c- TiO_x (dA) from the obtained data (Figs. 4 and 6). It is possible by the extraction of the length between lattice spacing peaks from the high-resolution TEM images (Fig. S3). Lattice parameter (dA) was estimated for different areas with a phase change indication. The obtained ratios of dA (3.421 Å, 3.16 Å, 2.841 Å) were compared to the literature results for deposited TiO_x films. The closest reported value is dA ~3.499–3.533 Å of the anatase phase A (101) of TiO_2, was deposited by pulsed laser deposition following annealing at 500 °C [27]. Furthermore, under question theory for the origin of passivation improvement for e-beam deposited TiO_x thin film and annealing affect might be related to chemical passivation. Chemical passivation theory represents an oxide growth in between the TiO_x and c-Si bulk, it forms the passivation of so-called "dangling bonds" on the Si surface [28].

In addition to the particular theory of chemical passivation of annealed thin TiO_x film, ellipsometry thickness measurements of SiO_x layer in between TiO_x and Si bulk were carried out for samples with the as-deposited and annealed TiO_x thin film. Certain thicknesses were deposited to observe if such parameter effects a passivation quality. It is widely reported that passivation or carrier selective layer TiO_x layers have high resistance [29–31]. Furthermore, composition of TiO_x layer

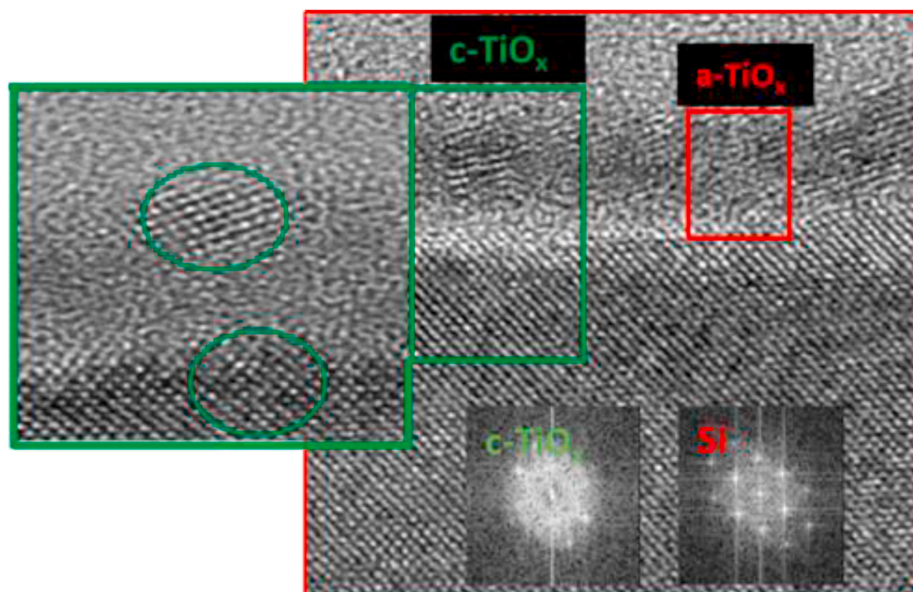

Fig. 4. High-resolution TEM images and diffraction peaks for detected *c*-TiO_x phase on the annealed at 550 °C TiO_x layer.

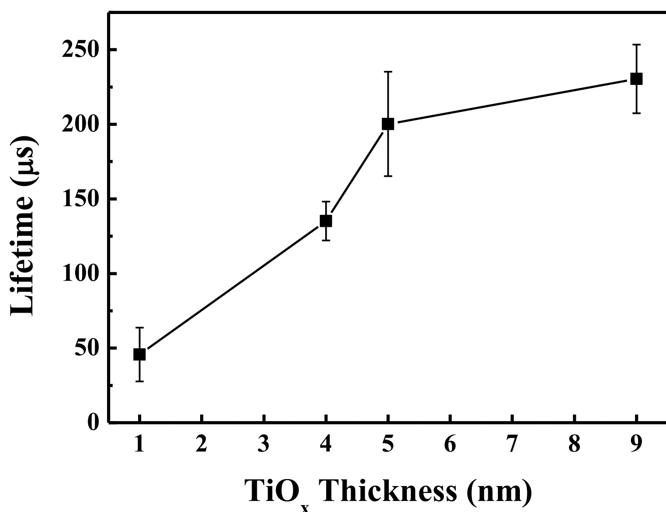

Fig. 5. Titanium oxide layer thickness as a function of MCLT measured for samples after the post-annealing procedure at 450 °C.

can vary with a thickness (oxygen-deficient structure) [32]. Hence, it is crucial to find a critical thickness at which optimal passivation and resistance parameter might be achieved.

To estimate co-relation between annealing temperature and TiO_x layer thickness, different TiO_x layer thicknesses were deposited. Following with the samples post-annealing at optimal temperature 450 °C and MCLT measure as presented in Fig. 3. A previously reported dependency of passivation performance on TiO_x thin films thickness was observed [33], according to Fig. 5 a trend-off between the passivation and the TiO_x film thickness is represented. Moreover, Fig. 6(c) represents increase in the thickness of SiO_x layer (a layer in-between titanium oxide and Si bulk) for all samples with TiO_x post-annealing process. According to under question theory, growth of SiO_x layer is produced by an oxygen withdrawn from the TiO_x layer, it results in improved chemical passivation of Si surface by SiO_x. Simultaneously an oxygen ratio in the TiO_x layer is decreased. Enhanced oxygen vacancies amount in the TiO_x might play the role of additional conductive centers [33,34]. On the other hand, an actual decrease of TiO_x thickness layers before and after the annealing process was not observed.

The thickness increase of SiO_x layer when compared to not annealed samples, was indicated by the EDS TEM image analysis and it is represented in Fig. 6(a), (b). Furthermore, conducted analysis revealed, an SiO_x layer increase after the annealing procedure, simultaneously TiO_x layer has remained constant thickness. Additionally, changes in oxygen composition of TiO_x layers are not drastic and only interface in between TiO_x/SiO_x is affected. Moreover, to notice oxygen withdrawn from the TiO_x layer an improved analysis and equipment are needed. It is equally important to admit that annealing procedure was conducted in a vacuum tube furnace with the forming gas flow (H_2 5% mixed in N_2 gas). Hence, SiO_x growth could not be affected by the external environment during the annealing process. As consequence, specific reaction mechanism is proposed and shown in Fig. 6(d).

According to the previously mentioned possible chemical origin for TiO_x thin films passivation, a coherent to our study theory is further introduced. Among possible chemical passivation origins, so-called field-effect passivation [35] is equally important for this study. It is

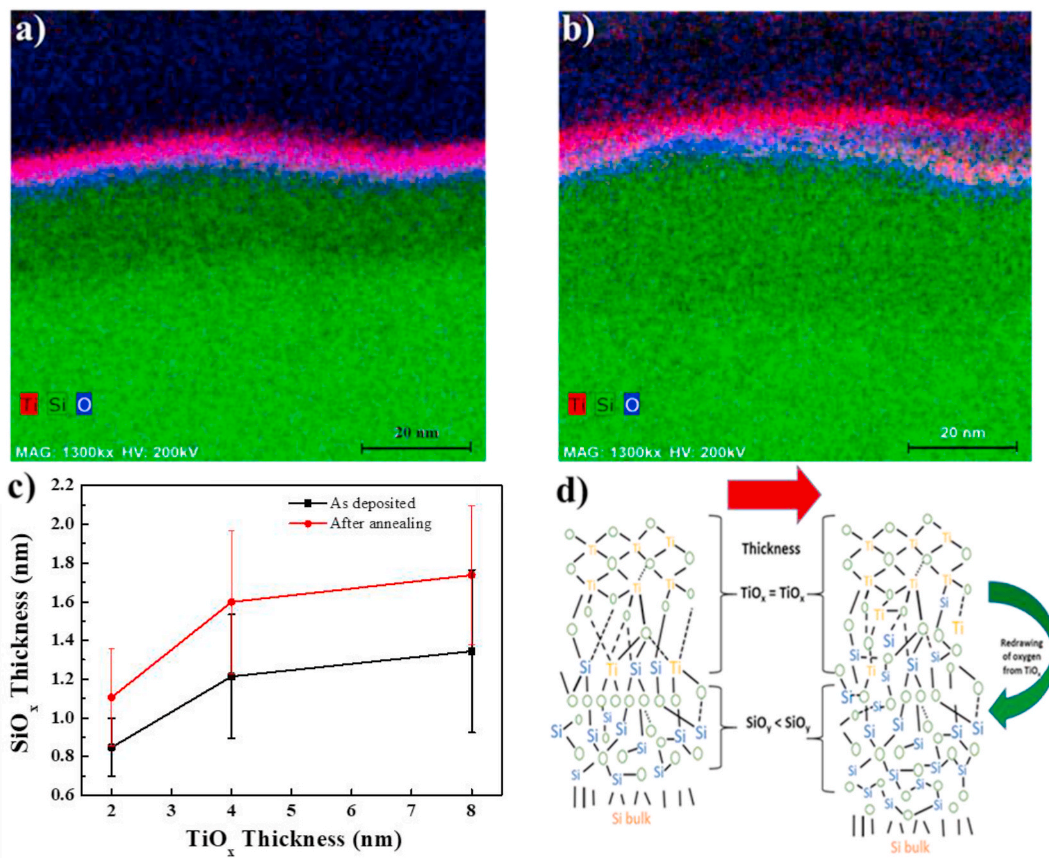

Fig. 6. a) b) TEM in-situ energy-dispersive X-ray spectroscopy (EDX) analysis of 4 nm TiOx film. a) as-deposited, b) after post-deposition annealing at 400 °C. c) Ellipsometry measurements result of the precise silicon oxide layer to TiO_x for different thickness, before and after the post-annealing process. d) Schematic of thermal reaction resulting in formation of additional silicon oxide (SiO_x) layer. (For interpretation of the references to colour in this figure legend, the reader is referred to the Web version of this article.)

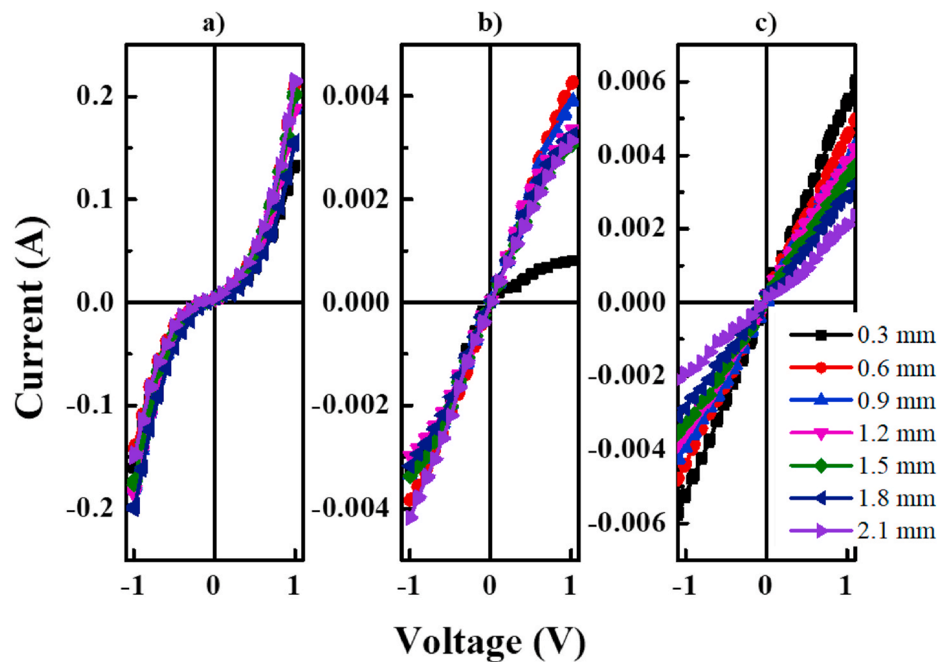

Fig. 7. Measured I–V curves for samples measured during TLM experiments, (a) annealed at 200 °C, (b) annealed at 300 °C (c) annealed at 400 °C, representing annealing affecting resistivity of TiO_x layer described in our work.

based on the band bending effect between TiO_x and c-Si. A band bending effect is coherent to the selective carrier properties of TiO_x, due to analysis of WF range for the deposited titanium oxide material. Thus, carrier selective materials have a variety of WF, this fact indicates them suitable for both hole and electron selective contacts. Consequently, a field-effect is caused by the carrier selective materials with a different WF, which are represented in Fig. 1(c).

From the previously performed TLM analysis a resistivity values of our material were obtained. A critical parameter for the TiO_x layer, as carrier selective contact is a specific contact resistivity (ρ_{spc}) was extracted. Correspondingly, a non-ohmic behavior for the I–V curves of the samples was observed in Fig. 7. A similar phenomenon of decreasing of TiO_x layer resistivity after the annealing process was reported other study [36]. Moreover, in analogy to the certain work, annealing procedure for our TiO_x thin films (5 nm) at different temperatures was conducted. Following the annealing experiment, I–V curves from the TLM analysis were obtained. Thus, resistivity slopes for different thicknesses of TiO_x thin films were plotted. An example of such slope is presented in Fig. S4 (additionally a graph of resistivity of TiO_x thin film as a function of transfer length is plotted. The I–V curves in Fig. 7 demonstrate an obvious difference between the sample's resistivity depending on the annealing temperature. Furthermore, I–V curves obtained for 300 °C annealed samples (Fig. 7(b)) indicated changes from non-Ohmic to Ohmic contact.

The specific contact resistivity was extracted for all cases, according to Eq. (4), values obtained from the calculation are indicated in Fig. S4. An approximate linear increase of contact resistivity with the thickness of TiO_x thin films is demonstrated. This resistivity trend demonstrates the ineffectiveness of depositing thicker layers of TiOx for passivation improvement in under question case. Hence, the resistivity increases linearly and a thicker layer of TiO_x can result in a dramatic resistivity increase in compare to the passivation performance. As a result, thicker TiO_x layers are not applicable as high efficiency carrier selective contacts. Thus, there is no further possibility to utilize e-beam deposited thicker TiO_x as passivation layers for c-Si solar cells.

A particular attention was dedicated to the annealing process of Al capping on TiO_x layers. This indicated dramatical conductivity improvement on samples annealed with TLM pad. Hence, it was discovered that annealing at 400 °C causes changes in the conductivity of the TiO_x thin film. Moreover, it is accepted in the semiconductor industry that a temperature of 400 °C and above is applied for the formation of ohmic contact between silicone and aluminum [37]. At this point, there is a need to produce reliable evidence of heat treatment does not cause Al penetration into the TiO_x layer, or the conductivity improvement is the result of another effect.

The work carried out demonstrates the possibility of potential improvement and further implementation of e-beam deposited titanium oxide thin layers as carrier selective contacts for c-Si solar cells. However, the thin layers of e-beam evaporated TiO_x in question have revealed serious drawbacks in comparison to the novel methods of deposition. Nonetheless, there are a few key points in achieving high passivation by E-deposited TiO_x, which is post-processing, such as heat treatment. A further crucial aspect is in deposition process conditions such as deposition rate, base or oxygen pressure. The thickness of the passivation TiO_x layer itself, in our case, plays an essential role in the subsequent solar cell fabrication, due to the tradeoff discovered between TiO_x layer thickness/passivation quality and resistivity. Hence, future fabrication of solar cell devices based on e-beam evaporated TiO_x as an alternative to ALD needs i) determination of optimal layer thickness ii) an improvement on the resistivity of such layers. As both parameters will affect a V_{oc} of the dopant free solar cell based on the TiO_x in question.

Annealing procedures of TiO_x are crucial, yet have drawbacks, such as crystal phase formation that caused at a specific temperature range. The passivation quality of annealed TiO_x layer is decreased at 550 °C degree in accordance with TEM analysis. Simultaneously, high-temperature treatment in inert atmosphere dramatically enhances passivation performance (Fig. 3). Another positive aspect of heat treatment is in the improvement of TiO_x layer conductivity in combination with a deposited Al layer.

As a result, a formation of additional SiO_x layer during the post-deposition processing improves passivation quality of e-beam deposited TiO_x layer. Moreover, a heat-treatment process of TiO_x has positive affect on conductivity increase or passivation improvement (300–450 °C). Hence, it is a valuable operation for further studies on CSC TiO_x, despite its drawbacks.

Equally important, this study achieved optimal conditions for the e-

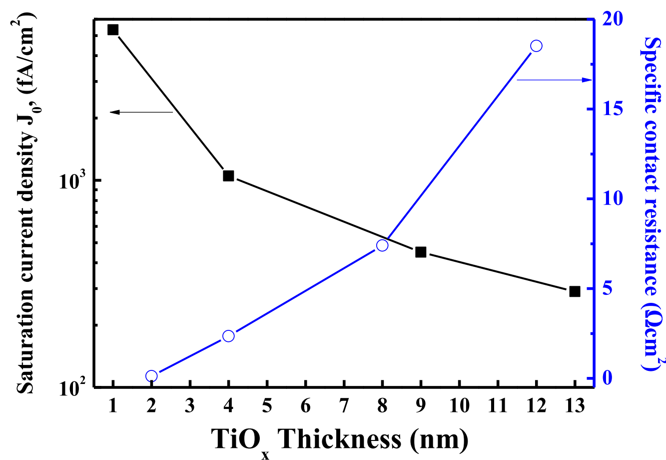

Fig. 8. TiOx passivation layer thickness as a function of specific contact resistance (ρ_{spc}) obtained as a result of TLM analysis.

beam deposition of TiO_x thin films for carrier selective and passivation properties. Fig. 8 represents a trade-off between the thickness of the TiO_x layer, J_0 and specific contact resistance. Furthermore, this work presents interesting findings for the processing of TiO_x e-beam deposition. Firstly – lower base pressure and a deposition rate provide higher passivation quality for TiO_x thin films. Secondly – enhanced passivation performance as a result of the annealing process on the TiO_x/Si stack with a thin SiO_x layer formed in between. According to the TEM analysis, the crystallization of TiO_x is initiated at 500 °C, at which point increased grain boundary is formed, thus negatively affecting passivation performance. Considering the trade-off between SRV and specific contact resistance (Fig. 8) which is dependent on the TiO_x thickness, we can estimate that a 4–9 nm thickness range has improved passivation quality. However, ρ_{spc} is almost gradually increased in contrast to SRV. In this case, 4 nm film of TiO_x is the optimal condition for further work with e-beam deposited TiO_x as CSC. Additionally, it is postulated that atmospheric process conditions such as base pressure and deposition rate are crucial for passivation performances of e-beam evaporated TiO_x. Secondly, the interfacial layer of SiO_x in between TiO_x and c-Si substrate plays one of the leading roles for enhanced passivation performance. Finally, the crystallization of the TiO_x layer is detrimental to passivation performance.

4. Conclusions

This study has presented work on the process of optimization for e-beam evaporated TiO_x thin films for selective electron contacts, despite the relatively low performance achieved by the TiO_x functional layers in question. However, the formation TiO_x based contacts by e-beam deposition is novel and has not been widely reported on. Our target was to achieve equal or higher values of J_0 and ρ_{spc} in comparison to ALD deposited TiO_x carrier selective layers ($J_0 < 102$ fA/cm^2, $\rho_{spc} < 10^{-2}$ Ω cm^2). Regarding the values obtained in the literature, for the ALD deposited 6 nm of TiO_x in Al/TiO_x/n-Si stack has achieved ρ_{spc} ~0.6 mΩ cm^2 [12], another ALD deposited case of the TiO_x with 3 nm thickness onto the previously thermally grown tunneling SiO_2 ~ 1.2 nm layer for additional passivation in the Al/TiO_x/SiO_2/n-Si stack has showed high performance SRV ~ 15 cm/s and ρ_{spc} ~ 26 mΩ cm^2 [38]. In our case e-beam deposited TiO_x on top of the native oxide (was formed during cleaning <1 nm) in Al/TiO_x/n-Si stack showed ρ_{spc} ~ 2.29 Ω/cm^2 which is 2 orders magnitude higher from the expected value and J_0 ~ 1016.64 fA/cm^2 – one order magnitude higher for the optimal thickness 4 nm. Whenever other techniques of TiO_x deposition such as CVD, PLD or sputtering showed poorer performance in comparison to our case. For example, CVD deposited TiO_x with 3 nm thickness showed SRV ~400 cm/s and J0 ~ 3247.29 fA/cm^2 [39]. Pulsed laser sputtered TiO_x demonstrated ρ_{spc} ~6 Ω cm^2 [40].

Under study, titanium oxide e-beam deposited selective carrier contacts have less potential in the c-Si solar cells industry in comparison to the newer deposition techniques (ALD, PECVD). However, this study reveals consistent findings for the improvement of e-beam deposited TiO_x CSC. E-beam evaporated TiO_x passivation layer has potential as a cost effective CSC for the dopant free c-Si cells, however needs further improvement to become competitive with ALD deposited TiO_x. Moreover, further combinations of TiO_x and deposited SiO_x thin layers with additional postprocessing as demonstrated in our work, might be a key solution for higher performance achievement.

Declaration of competing interest

The authors declare that they have no known competing financial interests or personal relationships that could have appeared to influence the work reported in this paper.

Acknowledgments

This work was supported by Korea Institute of Science and Technology (KIST), the National Research Foundation of Korea (NRF) (Grant No. NRF-2019K1A3A1A61091348), and the Korea Institute of Energy Technology Evaluation and Planning (KETEP) (Grant No. 20193091010460) funded by the Ministry of Trade, Industry & Energy (MOTIE).

Appendix A. Supplementary data

Supplementary data to this article can be found online at https://doi.org/10.1016/j.cap.2021.10.005.

References

[1] M. Xue, Y. Chen, J. Jia, Y. Huo, C.Y. Lu, K. Zang, K. Xu, Y.C. Huang, X. Chen, J. Harris, Titanium Oxide Contact Passivation Layer for Thin Film Crystalline Silicon Solar Cells, IEEE, 2016, pp. 2871–2873. PVSC, https://10.1109/PVSC.2016.7750179.
[2] K. Kukli, M. Ritala, M. Schuisky, M. Leskelä, T. Sajavaara, J. Keinonen, T. Uustare, A. Hårsta, Atomic layer deposition of titanium oxide from TiI4 and H2O2, Chem. Vap. Depos. 6 (6) (2000) 303–310, https://doi.org/10.1002/1521-3862(200011)6:6<303::AID-CVDE303>3.0.CO;2-J.
[3] National Renewable Energy Laboratory (NREL) Efficiency Chart, 2019.
[4] Jimmy Melskens, Bas WH. van de Loo, Bart Macco, Lachlan E. Black, Sjoerd Smit, W.M.M. Kessels, Passivating contacts for crystalline silicon solar cells: from concepts and materials to prospects, IEEE Journal of Photovoltaics 8 (2) (2018). https://10.1109/JPHOTOV.2018.2797106.
[5] Shadia J. Ikhmayies, Transparent Conducting Oxides for Solar Cell Applications. Mediterranean Green Buildings & Renewable Energy, Springer, Cham, 2017, pp. 899–907, https://doi.org/10.1007/978-3-319-30746-6_70.
[6] L.G. Gerling, S. Mahato, A. Morales-Vilches, G. Masmitja, P. Ortega, C. Voz, J. Puigdollers, Transition metal oxides as hole-selective contacts in silicon heterojunctions solar cells, Sol. Energy Mater. Sol. Cell. 145 (2016) 109–115, https://doi.org/10.1016/j.solmat.2015.08.028.
[7] J. BullocN, Y. Wan, Z. Xu, S. Essig, M. HetticN, H. Wang, A. Javey, Stable dopant-free asymmetric heterocontact silicon solar cells with efficiencies above, ACS Energy Letters 3 (3) (2018) 508–513. https://pubs.acs.org/doi/full/10.1021/acsenergylett.7b01279.
[8] X. Xu, Z. Liu, Z. Zuo, M. Zhang, Z. Zhao, Y. Shen, M. Wang, Hole selective NiO contact for efficient perovskite solar cells with carbon electrode, Nano Lett. 15 (4) (2015) 2402–2408, https://doi.org/10.1021/nl504701y, 2015.
[9] Hideo Hosono, Recent progress in transparent oxide semiconductors: materials and device application, Thin Solid Films 515 (15) (2007) 6000–6014, https://doi.org/10.1016/j.tsf.2006.12.125.
[10] S. Kashiwaya, J. Morasch, V. Streibel, T. Toupance, W. Jaegermann, A. Klein, The work function of TiO2, Surfaces 1 (1) (2018) 73–89, https://doi.org/10.3390/surfaces1010007.
[11] Yu Bai, Ivan Mora-Sero, Filippo De Angelis, Juan Bisquert, Peng Wang, Titanium dioxide nanomaterials for photovoltaic applications, Chem. Rev. 114 (2014) 19, https://doi.org/10.1021/cr400606n.
[12] T. Matsui, M. Bivour, P. Ndione, P. Hettich, M. Hermle, Investigation of atomic-layer-deposited TiOx as selective electron and hole contacts to crystalline silicon, Energy Procedia 124 (2017) 628–634, https://doi.org/10.1016/j.egypro.2017.09.093. Energy Procedia 124.
[13] R.R. César, A.D. Barros, I. Doi, J.A. Diniz, J.W. Swart, Thin titanium oxide films obtained by RTP and by sputtering, in: 29th Symposium on Microelectronics

Technology and Devices (SBMicro), 2014, pp. 1–4, https://doi.org/10.1109/SBMicro.2014.6940120. IEEE.
[14] S.G. Ullattil, P. Periyat, Sol-gel synthesis of titanium dioxide, in: Sol-Gel Materials for Energy, Environment and Electronic Applications, Springer, Cham, 2017, pp. 271–283, https://doi.org/10.1007/978-3-319-50144-4_9.
[15] V. Jokanović, B. Čolović, A.T. Petkoska, A. Mraković, B. Jokanović, M. Nenadović, I. Nasov, Optical properties of titanium oxide films obtained by cathodic arc plasma deposition, Plasma Sci. Technol. 19 (12) (2017) 125504, https://doi.org/10.1088/2058-6272/aa8806.
[16] P. Koswatta, M. Boccard, Z. Holman, Carrier-selective contacts in silicon solar cells, in: 2015 IEEE 42nd Photovoltaic Specialist Conference (PVSC), 2015, pp. 1–4, https://doi.org/10.1109/PVSC.2015.7356143. IEEE.
[17] M. Bivour, J. Temmler, H. Steinkemper, M. Hermle, Molybdenum and tungsten oxide: high work function wide band gap contact materials for hole selective contacts of silicon solar cells, Sol. Energy Mater. Sol. Cell. 142 (2015) 34–41, https://doi.org/10.1016/j.solmat.2015.05.031.
[18] M. Bivour, J. Temmler, F. Zähringer, S. Glunz, M. Hermle, High work function metal oxides for the hole contact of silicon solar cells, IEEE 43rd Photovoltaic Specialists Conference (PVSC) (2016), https://doi.org/10.1109/PVSC.2016.7749581, 0215-0220.
[19] M.H. Park, Y.J. Jang, H.M. Sung-Suh, M.M. Sung, Selective atomic layer deposition of titanium oxide on patterned self-assembled monolayers formed by microcontact printing, Langmuir 20 (6) (2004) 2257–2260, https://doi.org/10.1021/la035760c.
[20] Charles Bishop, Vacuum Deposition onto Webs, Films and Foils, William Andrew, 2011.
[21] Z. Ling, J. He, X. He, M. Liao, P. Liu, Z. Yang, P. Gao, Excellent passivation of silicon surfaces by thin films of electron-beam-processed titanium dioxide, IEEE Journal of Photovoltaics 7 (6) (2017) 1551–1555, https://doi.org/10.1109/JPHOTOV.2017.2749975.
[22] M. Xue, R. Islam, Y. Chen, J. Chen, C.Y. Lu, A. Mitchell Pleus, J.S. Harris, Carrier-selective interlayer materials for silicon solar cell contacts, J. Appl. Phys. 123 (14) (2018) 143101, https://doi.org/10.1063/1.5020056.
[23] S.M. Sze, K.K. Ng, Physics of Semiconductor Devices, John Wiley & Sons, 2006.
[24] S. Andersson, B. Collén, U. Kuylenstierna, A. Magnéli, Phase analysis studies on the titanium-oxygen system, Acta chem. scand 11 (10) (1957) 1641–1652.
[25] D.A. Hanaor, C.C. Sorrell, Review of the anatase to rutile phase transformation, J. Mater. Sci. 46 (4) (2011) 855–874, https://doi.org/10.1007/s10853-010-5113-0.
[26] S. Wu, X. Luo, Y. Long, B. Xu, Exploring the phase transformation mechanism of titanium dioxide by high temperature in situ method, in: IOP Conference Series: Materials Science and Engineering, 493, IOP Publishing, 2019, https://doi.org/10.1088/1757-899X/493/1/012010. No. 1, p. 012010.
[27] S.S. Al-Obaidi, A.A. Yousif, Synthesis of nanostructured TiO2 thin films by pulsed laser deposition (PLD) and the effect of annealing temperature on structural and morphological properties, Ibn AL-Haitham Journal For Pure and Applied Science 26 (3) (2017) 143–152.
[28] E. Cartier, J.H. Stathis, D.A. Buchanan, Passivation and depassivation of silicon dangling bonds at the Si/SiO2 interface by atomic hydrogen, Appl. Phys. Lett. 63 (11) (1993) 1510–1512, https://doi.org/10.1063/1.110758.
[29] A. Yildiz, S.B. Lisesivdin, M. Kasap, D. Mardare, Electrical properties of TiO2 thin films, J. Non-Cryst. Solids 354 (45–46) (2008) 4944–4947, https://doi.org/10.1016/j.jnoncrysol.2008.07.009.
[30] D. Brassard, D.K. Sarkar, M.A. El Khakani, L. Ouellet, Tuning the electrical resistivity of pulsed laser deposited TiSiO x thin films from highly insulating to conductive behaviors, Appl. Phys. Lett. 84 (13) (2004) 2304–2306, https://doi.org/10.1063/1.1688999.
[31] C. Lee, S. Bae, H. Park, D. Choi, H. Song, H. Lee, H.S. Lee, Properties of thermally evaporated titanium dioxide as an electron-selective contact for silicon solar cells, Energies 13 (3) (2020) 678, https://doi.org/10.3390/en13030678.
[32] I. Vaquila, M.C.G. Passeggi, J. Ferrón, Oxidation process in titanium thin films, Phys. Rev. B 55 (20) (1997) 13925, https://doi.org/10.1103/PhysRevB.55.13925.
[33] J. Nowotny, A. Malik, M.A. Alim, T. Bak, A.J. Atanacio, Electrical properties and defect chemistry of indium-doped TiO2: electrical conductivity, ECS Journal of Solid State Science and Technology 3 (10) (2014) P330, https://doi.org/10.1007/s11581-014-1351-5.
[34] B. Bharti, S. Kumar, H.N. Lee, R. Kumar, Formation of oxygen vacancies and Ti 3+ state in TiO 2 thin film and enhanced optical properties by air plasma treatment, Sci. Rep. 6 (1) (2016) 1–12, https://doi.org/10.1038/srep32355.
[35] R.S. Bonilla, P.R. Wilshaw, Stable field effect surface passivation of n-type Cz silicon, Energy Procedia 38 (2013) 816–822, https://doi.org/10.1016/j.egypro.2013.07.351.
[36] A.S. Bakri, M.Z. Sahdan, F. Adriyanto, N.A. Raship, N.D.M. Said, S.A. Abdullah, M. S. Rahim, Effect of annealing temperature of titanium dioxide thin films on structural and electrical properties, in: AIP Conference Proceedings, 1788, AIP Publishing LLC, 2017, https://doi.org/10.1063/1.4968283. No. 1, p. 030030.
[37] L.A. Kosyachenko (Ed.), Solar Cells: Silicon Wafer-Based Technologies, BoD–Books on Demand, 2011.
[38] X. Yang, K. Weber, Z. Hameiri, S. De Wolf, Industrially feasible, dopant-free, carrier-selective contacts for high-efficiency silicon solar cells, Prog. Photovoltaics Res. Appl. 25 (11) (2017) 896–904, https://doi.org/10.1002/pip.2901.
[39] K.A. Nagamatsu, S. Avasthi, G. Sahasrabudhe, G. Man, J. Jhaveri, A.H. Berg, J. C. Sturm, Titanium dioxide/silicon hole-blocking selective contact to enable double-heterojunction crystalline silicon-based solar cell, Appl. Phys. Lett. 106 (12) (2015) 123906, https://doi.org/10.1063/1.4916540.
[40] T. Hitosugi, N. Yamada, S. Nakao, Y. Hirose, T. Hasegawa, Properties of TiO2-based transparent conducting oxides, Phys. Status Solidi 207 (7) (2010) 1529–1537, https://doi.org/10.1002/pssa.200983774.